minerals

MDPI

Article

Tamuraite, $Ir_5Fe_{10}S_{16}$, a New Species of Platinum-Group Mineral from the Sisim Placer Zone, Eastern Sayans, Russia

Andrei Y. Barkov [1,*], Nadezhda D. Tolstykh [2], Robert F. Martin [3] and Andrew M. McDonald [4]

[1] Research Laboratory of Industrial and Ore mineralogy, Cherepovets State University, 5 Lunacharsky Avenue, 162600 Cherepovets, Russia
[2] V.S. Sobolev Institute of Geology and Mineralogy, Siberian Branch of the Russian Academy of Science, 3 Avenue Prospekt Koptyuga, 630090 Novosibirsk, Russia; tolst@igm.nsc.ru
[3] Department of Earth and Planetary Sciences, McGill University, 3450 University Street, Montreal, QC H3A 0E8, Canada; robert.martin@mcgill.ca
[4] Harquail School of Earth Sciences, Laurentian University, 935 Ramsey Lake Road, Sudbury, ON P3E 2C6, Canada; amcdonald@laurentian.ca
* Correspondence: ore-minerals@mail.ru; Tel.: +7-8202-55-65-97

Abstract: Tamuraite, ideally $Ir_5Fe_{10}S_{16}$, occurs as discrete phases (≤20 μm) in composite inclusions hosted by grains of osmium (≤0.5 mm across) rich in Ir, in association with other platinum-group minerals in the River Ko deposit of the Sisim Placer Zone, southern Krasnoyarskiy Kray, Russia. In droplet-like inclusions, tamuraite is typically intergrown with Rh-rich pentlandite and Ir-bearing members of the laurite–erlichmanite series (up to ~20 mol.% "IrS_2"). Tamuraite is gray to brownish gray in reflected light. It is opaque, with a metallic luster. Its bireflectance is very weak to absent. It is nonpleochroic to slightly pleochroic (grayish to light brown tints). It appears to be very weakly anisotropic. The calculated density is 6.30 g·cm^{-3}. The results of six WDS analyses are Ir 29.30 (27.75–30.68), Rh 9.57 (8.46–10.71), Pt 1.85 (1.43–2.10), Ru 0.05 (0.02–0.07), Os 0.06 (0.03–0.13), Fe 13.09 (12.38–13.74), Ni 12.18 (11.78–13.12), Cu 6.30 (6.06–6.56), Co 0.06 (0.04–0.07), S 27.23 (26.14–27.89), for a total of 99.69 wt %. This composition corresponds to $(Ir_{2.87}Rh_{1.75}Pt_{0.18}Ru_{0.01}Os_{0.01})_{\Sigma 4.82}(Fe_{4.41}Ni_{3.90}Cu_{1.87}Co_{0.02})_{\Sigma 10.20}S_{15.98}$, calculated based on a total of 31 atoms per formula unit. The general formula is $(Ir,Rh)_5(Fe,Ni,Cu)_{10}S_{16}$. Results of synchrotron micro-Laue diffraction studies indicate that tamuraite is trigonal. Its probable space group is $R\bar{3}m$ (#166), and the unit-cell parameters are a = 7.073(1) Å, c = 34.277(8) Å, V = 1485(1) Å^3, and Z = 3. The c:a ratio is 4.8462. The strongest eight peaks in the X-ray diffraction pattern [d in Å(hkl)(I)] are: 3.0106(2$\bar{1}$6)(100), 1.7699(4$\bar{2}$0)(71), 1.7583(20$\underline{1}$6)(65), 2.7994(205)(56), 2.9963(10$\underline{1}$0)(50), 5.7740(10$\bar{2}$)(45), 3.0534(20$\bar{1}$)(43) and 2.4948(208)(38). The crystal structure is derivative of pentlandite and related to that of oberthürite and torryweiserite. Tamuraite crystallized from a residual melt enriched in S, Fe, Ni, Cu, and Rh; these elements were incompatible in the Os–Ir alloy that nucleated in lode zones of chromitites in the Lysanskiy layered complex, Eastern Sayans, Russia. The name honors Nobumichi Tamura, senior scientist at the Advanced Light Source of the Lawrence Berkeley National Laboratory, Berkeley, California.

Keywords: tamuraite; platinum-group mineral; PGE sulfide; iridium–iron sulfide; Sisim Placer Zone; River Ko deposit; Lysanskiy layered complex; Eastern Sayans; Russia

Citation: Barkov, A.Y.; Tolstykh, N.D.; Martin, R.F.; McDonald, A.M. Tamuraite, $Ir_5Fe_{10}S_{16}$, a New Species of Platinum-Group Mineral from the Sisim Placer Zone, Eastern Sayans, Russia. *Minerals* **2021**, *11*, 545. https://doi.org/10.3390/min11050545

Academic Editor: Ulf Hålenius

Received: 18 April 2021
Accepted: 17 May 2021
Published: 20 May 2021

1. Introduction

Tamuraite, a new mineral species of ideal composition $Ir_5Fe_{10}S_{16}$, was found in a placer along the River Ko, south of Krasnoyarsk, Russia (approximate location 54°47′ N, 93°16′ E). The heavy-mineral fraction recovered from the River Ko deposit and the placer in the neighboring River Seyba is mainly derived from ultramafic units of the Lysanskiy layered complex, Eastern Sayans, Russia [1–3]. The development of placers bearing platinum-group minerals (PGM) corresponds to the Sisim river system in the

southern portion of Krasnoyarskiy Kray in South Central Siberia (Figure 1a,b). Our aims are to describe the mode of occurrence, associations and properties of tamuraite. The mineral and its name were approved (IMA 2020-098) by the Commission on New Minerals, Nomenclature and Classification (CNMNC) of the International Mineralogical Association.

Figure 1. Location of the River Ko placer deposit, which forms part of the Sisim Placer Zone, in the Krasnoyarskiy Kray of the Russian Federation (**a**). Geological sketch-map shows the distribution of the main massifs (after [4], and references therein) in the placer area, which is drained by the rivers Ko and Seyba, tributaries of the River Sisim (**b**).

2. Geological Context, Materials and Methods

Hundreds of placers grains were collected and investigated at different times in the River Sisim Placer Zone [1–3]. Grains of tamuraite form part of roundish composite inclusions of sulfide minerals rich in platinum-group elements (PGE); the polymineralic inclusions are hosted by Os–Ir alloy grains. Many of the main massifs exposed in the area investigated and shown schematically in Figure 1b ([4], and references therein) are composed dominantly of bodies of granite and granodiorite (namely Arzybeiskiy, Angulskiy, Derbinskiy and Kanzubinskiy, among others), peralkaline granite (Okunevskiy), members of the gabbro–diorite–granodiorite (Shindinskiy, Olkhovsko-Chibizhekskiy) and gabbro–monzonite–syenite associations (e.g., Buedzhinskiy). None of these can be considered as the potential provenance of the PGM-bearing placer studied at River Ko. In the vicinity, two igneous complexes contain abundant ultramafic units: (1) the clinopyroxenite–gabbro–anorthosite suite of the Kulibinskiy layered complex (i.e., Kuvaiskiy and Shirokologskiy massifs) and (2) the dunite–peridotite–gabbro series of the Lysanskiy layered complex (Figure 1b). The latter is especially pertinent; it is large, composed mainly of three blocks (Lysanskiy, Podlysanskiy and Kedranskiy, ~0.5 km × 30 km in extent overall), and along with smaller fragmented bodies (Figure 1b). The complex displays tectonic contacts with the host rocks of the Bakhtinskaya suite of upper Proterozoic age; this suite comprises various basalts, andesitic basalts and volcanic tuff. The complex is formed of alternating sequences of serpentinite, wehrlite, lherzolite, harzburgite, clinopyroxenite, websterite, gabbronorite, troctolite, gabbro, and anorthosite. Some massifs of this complex are dominantly ultrabasic, and others contain mostly basic rocks. The complex hosts abundant Ti–(V) mineralization and podiform deposits of ilmenite—titanian magnetite ores. This complex was previously considered to represent the source rocks for the PGM-bearing placers associated with the Sisim zone [3].

Electron-microprobe analyses of tamuraite and the host grains of the alloy were conducted at McGill University using wavelength-dispersive spectrometry (WDS) using a JEOL JXA 8900 L instrument operated at 20 kV 20 nA, with a beam diameter set at 3 μm. The following X-ray lines were used: Cu$L\alpha$, Ni$K\alpha$, Fe$K\alpha$, Co$K\alpha$, Ir$L\alpha$, Rh$L\alpha$, Pt$L\alpha$, Pd$L\beta$,

Os$M\alpha$, Ru$L\alpha$ and S$K\alpha$. Counting times were 20 s on the peak. The Phi–Rho–Z method of corrections was applied. The peak-overlap corrections included Fe → Co, Os → Ir, Ru → Pd, Ir → Pt, and Ru → Rh corrections. The standards used were pure metals for the platinum-group elements, Fe, Cu, Co, and synthetic pentlandite for Ni and S. Values of standard deviations (σ) are ≤0.2 for Ir, Pt, and Cu, ≤0.1 for Ru, Os, Fe, and Ni, and ≤0.05 for Rh, Co and S.

Tiny grains of Rh-rich pentlandite and members of the laurite–erlichmanite series that coexist with tamuraite were analyzed via quantitative energy-dispersive spectrometry (EDS), at 20 kV and 1.6 nA, using a MIRA 3 LMU (Tescan Orsay Holding) scanning electron microscope equipped with an INCA Energy 450 XMax 80 (Oxford Instruments Nanoanalysis, UK) microanalysis energy-dispersive system at the Analytical Center for multi-elemental and isotope studies, SB RAS, Novosibirsk, Russia. The following X-ray lines were used: Cu$K\alpha$, Ni$K\alpha$, Fe$K\alpha$, Co$K\alpha$, Ir$L\alpha$, Rh$L\alpha$, Pt$L\alpha$ and S$K\alpha$. Minimum detection limits (3σ criterion) are ≤0.2 wt % for S, Fe, Co, Ni, Cu; ≤0.4 wt % for Rh; ≤0.5–0.7 wt % for Ir. The analytical error for the main components did not exceed 1–2 relative% and satisfied the requirements for quantitative analysis. Specimens of certified standards were used: FeS_2 and pure metals. Other details of the analytical techniques applied were summarized in [5].

Synchrotron micro-Laue diffraction studies, followed by monochromator energy scans, were performed using the beamline 12.3.2 on the holotype specimens of tamuraite at the Advanced Light Source (ALS) of the Lawrence Berkeley National Laboratory, Berkeley, California, USA. The Laue diffraction patterns were collected with a PILATUS 1 M area detector using reflection geometry. The patterns were analyzed and indexed using XMAS v.6 following the procedure of Tamura (2014) [6].

3. Results

3.1. Mode of Occurrence and Associated Minerals

The grains of tamuraite (≤20 μm; Figure 2a–d, Figure 3a,b) occur with Rh-rich pentlandite and cavernous grains of laurite–erlichmanite solid solution in droplet-like polymineralic inclusions (≤50 μm). These platinum-group minerals (PGM) are hosted by placer grains of the Ir-bearing native Os (Figures 2a–d and 3a,b; Table 1), which corresponds to the mineral osmium [7]. Native Ir is also observed, but in subordinate quantities. Alloy grains of rutheniridosmine composition are rare. The composition of the alloys in the entire Sisim–Ko–Seyba placer area is limited to the Ru-poor portion of the system Os–Ir–Ru by the line Ru:Ir = 1 [3].

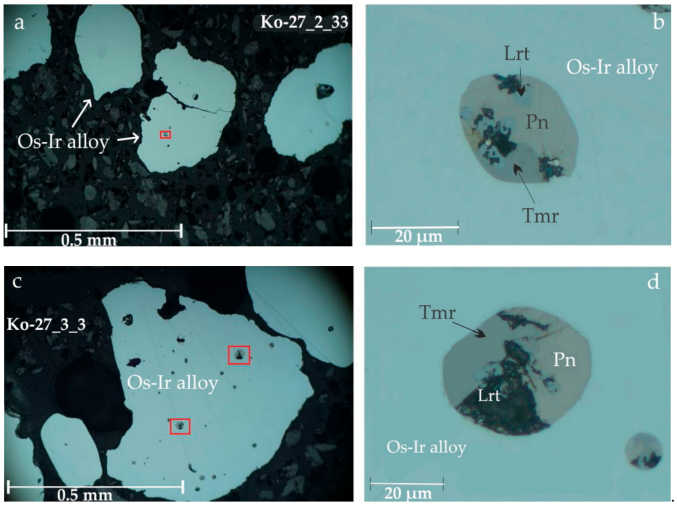

Figure 2. (**a**–**d**) Optical photographs of grains of the Os–Ir alloy; these host roundish polymineralic inclusions of tamuraite (Tmr), Rh-rich pentlandite (Pn) and members of the laurite–erlichmanite series (Lrt).

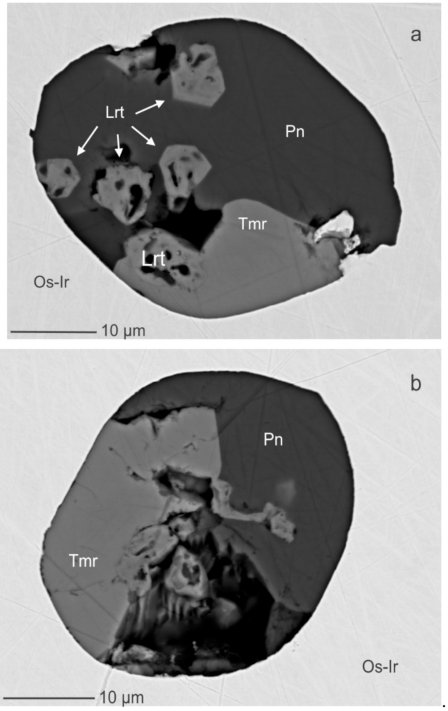

Figure 3. (**a**,**b**) Back-scattered electron images showing inclusions of platinum-group minerals. These are hosted by placer grains of Os–Ir–(Ru) alloy, labeled Os–Ir (i.e., the mineral osmium rich in Ir). Tamuraite (Tmr) is intimately associated with Rh-bearing pentlandite (Pn) and a member of the laurite–erlichmanite series (Lrt).

Table 1. Compositions of the Os–Ir alloy from the River Ko deposit in the Sisim Placer Zone.

#	Ir	Rh	Pd	Pt	Ru	Os	Fe	Ni	Total
(wt %)									
1	42.32	0.21	bdl	0.44	4.73	51.70	0.20	bdl	99.61
2	42.45	0.19	0.06	0.25	4.56	52.57	0.17	0.03	100.29
3	42.25	0.24	bdl	0.29	2.97	53.68	0.24	0.02	99.70
4	43.61	0.21	0.03	0.52	6.05	49.36	0.17	0.04	100.00
5	43.84	0.21	bdl	0.45	6.00	48.71	0.29	0.02	99.53
6	42.19	0.18	bdl	0.20	7.62	49.05	0.21	0.05	99.48
7	35.70	0.19	0.03	0.47	5.27	57.57	0.21	bdl	99.43
8	30.38	0.20	bdl	0.41	5.51	63.47	0.12	0.03	100.11
9	35.80	0.19	0.07	0.08	3.25	60.00	0.16	bdl	99.56
(at %)									
#	**Ir**	**Rh**	**Pd**	**Pt**	**Ru**	**Os**	**Fe**	**Ni**	**Total**
1	40.28	0.37	0.00	0.41	8.56	49.72	0.66	0.00	100
2	40.19	0.34	0.10	0.23	8.21	50.29	0.55	0.09	100
3	40.72	0.43	0.00	0.28	5.44	52.27	0.80	0.06	100
4	40.88	0.37	0.05	0.48	10.79	46.76	0.55	0.12	100
5	41.21	0.37	0.00	0.42	10.73	46.27	0.94	0.06	100
6	39.19	0.31	0.00	0.18	13.46	46.03	0.67	0.15	100
7	33.84	0.34	0.05	0.44	9.50	55.14	0.69	0.00	100
8	28.58	0.35	0.00	0.38	9.86	60.34	0.39	0.09	100
9	34.52	0.34	0.12	0.08	5.96	58.45	0.53	0.00	100

Note: Compositions #1–9 (WDS data) pertain to placer grains of osmium, the Os–Ir alloy, the host inclusions of tamuraite. Cobalt and Cu were sought but not detected.

The pentlandite in the droplet-shaped inclusions is invariably enriched in Rh, with minor amounts of Ir, Pd, other PGE, Cu and Co. Interestingly, the observed content of

Rh is relatively constant and close to ~1 apfu (Table 2). This feature is reminiscent of the synthesis of the pentlandite-type phase $Rh(Ni_4Fe_4)S_8$ at 700 °C, along with other $Fe_4Ni_4MS_8$ compounds (M = Ru, Pd) [8]. Rhodium is not associated with Co in compositions of the grains analyzed in the River Ko suite, in contrast to specimens of Rh–Co-bearing pentlandite from the River Bolshoy Khailyk deposit, in western Sayans, Russia, in which Rh and Co enter solid solution and substitute for Fe, not Ni, via a coupled mechanism of substitution: $Rh^{3+} + Co^{3+} + \square \rightarrow 3\ Fe^{2+}$ [9]. Several occurrences of PGE-rich pentlandite have been reported ([10,11] and references therein).

Table 2. Compositions of inclusions of pentlandite enriched in Rh from the River Ko deposit in the Sisim Placer Zone.

#	Ir	Rh	Pd	Ru	Os	Fe	Ni	S	Total (wt %)
1	bdl	10.68	bdl	bdl	bdl	23.58	30.38	30.89	95.53
2	bdl	10.69	bdl	bdl	bdl	23.69	30.31	30.88	95.57
3	bdl	5.42	1.25	bdl	bdl	24.82	31.37	31.75	94.61
4	bdl	11.81	bdl	bdl	bdl	24.56	29.43	31.06	96.86
5	bdl	11.57	bdl	bdl	bdl	24.23	29.02	30.65	95.47
6	1.82	12.28	bdl	bdl	bdl	23.13	27.68	30.99	96.80
7	bdl	10.66	bdl	bdl	0.94	26.22	26.38	32.88	99.05
8	bdl	11.06	bdl	bdl	bdl	25.77	28.29	31.92	97.04
9	bdl	10.30	bdl	bdl	bdl	26.33	27.99	31.10	95.72
10	bdl	7.64	2.03	bdl	1.08	29.97	26.13	31.83	99.58
11	bdl	7.19	bdl	1.19	bdl	24.46	30.47	31.26	94.57
12	0.95	10.42	bdl	1.64	bdl	23.35	28.24	30.60	95.20
13	bdl	10.87	bdl	bdl	0.89	24.81	29.69	31.56	97.82
14	bdl	10.68	bdl	bdl	bdl	24.39	29.41	30.79	95.27
15	bdl	11.74	bdl	1.25	bdl	21.17	31.87	30.76	96.79
16	bdl	11.45	bdl	bdl	bdl	21.14	31.87	31.09	95.55
17	bdl	8.55	bdl	2.05	bdl	21.96	32.87	31.42	96.85
18	bdl	8.63	bdl	1.88	bdl	21.66	33.02	30.67	95.86
19	bdl	8.86	bdl	bdl	bdl	23.19	31.91	31.00	94.96
20	bdl	9.25	bdl	2.56	bdl	22.36	31.32	31.40	96.89
Atoms per formula unit (apfu)									
#	Ir	Rh	Pd	Ru	Os	Fe	Ni	ΣPGE	ΣMe	S
1	0.00	0.88	0.00	0.00	0.00	3.58	4.38	0.88	8.84	8.16
2	0.00	0.88	0.00	0.00	0.00	3.59	4.37	0.88	8.84	8.16
3	0.00	0.44	0.10	0.00	0.00	3.72	4.47	0.54	8.72	8.28
4	0.00	0.96	0.00	0.00	0.00	3.69	4.21	0.96	8.87	8.13
5	0.00	0.96	0.00	0.00	0.00	3.69	4.21	0.96	8.86	8.14
6	0.08	1.02	0.00	0.00	0.00	3.53	4.02	1.10	8.76	8.24
7	0.00	0.85	0.00	0.00	0.04	3.83	3.67	0.89	8.63	8.37
8	0.00	0.89	0.00	0.00	0.00	3.83	4.00	0.89	8.73	8.27
9	0.00	0.84	0.00	0.00	0.00	3.97	4.02	0.84	8.83	8.17
10	0.00	0.60	0.16	0.00	0.05	4.37	3.62	0.81	8.92	8.08
11	0.00	0.59	0.00	0.10	0.00	3.70	4.38	0.69	8.77	8.23
12	0.04	0.87	0.00	0.14	0.00	3.60	4.14	1.05	8.79	8.21
13	0.00	0.88	0.00	0.00	0.04	3.69	4.21	0.92	8.82	8.18
14	0.00	0.88	0.00	0.00	0.00	3.71	4.25	0.88	8.84	8.16
15	0.00	0.97	0.00	0.10	0.00	3.21	4.60	1.07	8.88	8.12
16	0.00	0.94	0.00	0.00	0.00	3.21	4.61	0.94	8.77	8.23
17	0.00	0.69	0.00	0.17	0.00	3.28	4.67	0.86	8.82	8.18
18	0.00	0.71	0.00	0.16	0.00	3.28	4.76	0.87	8.91	8.09
19	0.00	0.73	0.00	0.00	0.00	3.51	4.59	0.73	8.83	8.17
20	0.00	0.75	0.00	0.21	0.00	3.36	4.47	0.97	8.79	8.21

Note: results of quantitative SEM/EDS analyses are expressed in weight% and in values of atoms per formula unit (apfu) calculated for a total of 17 apfu. Results of analyses #6, 7 include 0.90 and 1.97 wt % Cu, or 0.12 and 0.25 apfu, respectively. Composition #10 includes 0.90 wt % Co (i.e., 0.12 apfu). Platinum was not detected; bdl: below the detection limits. Relatively low totals are due to insufficient volumes of the analyzed grain.

The members of the laurite–erlichmanite series in the tamuraite-bearing globules display notable compositional variations (Table 3, Figure 4a–c). The covariation trends observed are similar to those already reported for the Sisim placers [3]. A relative enrichment in Ir (up to 0.2 apfu) is recorded. The Ir–Os correlation is positive, with a value of the correlation coefficient R = 0.83, based on 31 data points (quantitative SEM/EDS data; Figure 4c). The inverse Ru–Os correlation (Figure 4a) is accompanied by a negative Ru–Ir correlation (R = −0.90; Figure 4b). These findings are consistent with a scheme previously inferred: $(Os^{2+} + 2Ir^{3+} + \square) \rightarrow 4Ru^{2+}$ [3], or with $(Os^{2+} + Ir^{2+}) \rightarrow 2Ru^{2+}$, an alternative that seems less likely. Other mechanisms controlling incorporating Ir into the laurite–erlichmanite solid solution involve a sulfarsenide component [12,13]. The limited nature of the $[Ir_x(Ru,Os)_{1-x}]S_2$ solid solutions is well recognized in nature. A continuous and complete series of solid solutions exist between the RuS_2 and OsS_2 end-members (the laurite–erlichmanite series), whereas the "IrS_2" content is typically less than 20 mol.% [14]. The maximum extent of Ir appears to be documented in erlichmanite at Rudnaya, western Sayans, Russia: $(Os_{0.59}Ir_{0.35}Ru_{0.09})_{\Sigma 1.03}(S_{1.94}As_{0.03})_{\Sigma 1.97}$ [13]. The inferred limit is likely a result of vacancy-type defects and related complications arising from incorporating Ir [12].

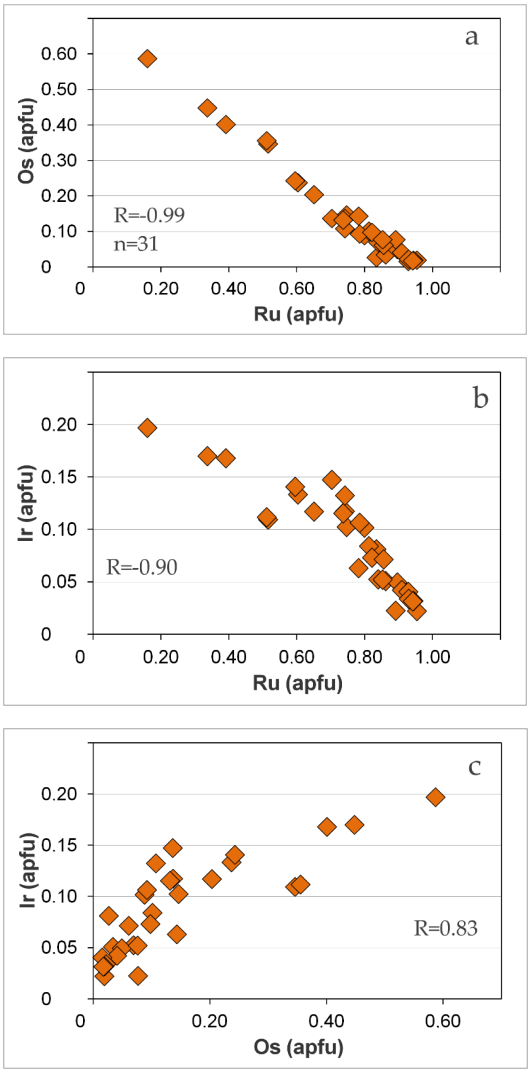

Figure 4. Correlations of Ru vs. Os (**a**), Ru vs. Ir (**b**) and Os vs. Ir (**c**) observed in members of the laurite–erlichmanite series at River Ko, Eastern Sayans, plotted in terms of atoms per formula unit (apfu) calculated for a total of 3 apfu. The correlation coefficient (R) was calculated based on 31 data points (n = 31).

Table 3. Compositions of inclusions of the laurite–erlichmanite series from the River Ko deposit in the Sisim Placer Zone.

#	Ir	Ru	Os	Fe	Ni	S	As	Total
(wt %)								
1	8.73	47.27	2.82	0.77	0.96	36.02	bdl	96.57
2	5.67	47.75	7.41	0.58	1.03	35.87	bdl	98.31
3	5.59	50.02	3.66	1.22	0.89	36.27	bdl	98.31
4	12.67	28.22	21.69	bdl	0.39	28.18	4.68	95.83
5	10.31	39.61	14.60	bdl	bdl	33.74	bdl	98.26
6	11.73	38.98	13.53	bdl	bdl	33.44	bdl	97.68
7	6.37	41.62	14.35	bdl	bdl	33.95	bdl	96.29
8	5.30	50.70	5.23	bdl	bdl	35.98	bdl	97.21
9	10.38	42.85	8.89	bdl	bdl	34.2	bdl	96.32
10	8.72	44.36	10.41	bdl	bdl	34.68	bdl	98.17
11	10.94	42.42	9.38	bdl	bdl	34.56	bdl	97.30
12	2.43	50.67	8.22	0.50	bdl	35.73	0.45	98.00
13	7.60	44.89	10.04	bdl	bdl	34.8	bdl	97.33
14	4.54	51.61	4.33	bdl	bdl	36.13	bdl	96.61
15	7.55	47.61	6.33	bdl	bdl	35.5	bdl	96.99
16	11.36	33.25	19.57	bdl	bdl	31.25	3.73	99.16
17	2.46	55.95	2.06	bdl	bdl	37.3	bdl	97.77
18	13.01	38.34	10.46	bdl	bdl	31.91	2.85	96.57
19	4.47	54.21	1.67	bdl	bdl	37.32	bdl	97.67
20	14.22	35.73	13.03	bdl	bdl	31.02	3.3	97.30
21	3.79	54.89	2.44	bdl	bdl	37.76	bdl	98.88
22	11.38	38.16	12.81	bdl	bdl	32.2	2.25	96.80
23	3.56	55.81	2.07	bdl	0.30	37.44	bdl	99.18
24	3.54	55.93	1.91	bdl	0.47	37.58	bdl	99.43
25	5.51	47.50	7.99	bdl	0.35	35.46	bdl	96.81

				(apfu)					
#	**Ir**	**Ru**	**Os**	**Fe**	**Ni**	**S**	**As**	**ΣMe**	**S + As**
1	0.08	0.83	0.03	0.02	0.03	2.00	0.00	1.00	2.00
2	0.05	0.84	0.07	0.02	0.03	1.99	0.00	1.01	1.99
3	0.05	0.86	0.03	0.04	0.03	1.97	0.00	1.03	1.97
4	0.14	0.60	0.24	0.00	0.01	1.87	0.13	0.99	2.01
5	0.10	0.75	0.15	0.00	0.00	2.00	0.00	1.00	2.00
6	0.12	0.74	0.14	0.00	0.00	2.00	0.00	1.00	2.00
7	0.06	0.78	0.14	0.00	0.00	2.01	0.00	0.99	2.01
8	0.05	0.90	0.05	0.00	0.00	2.01	0.00	0.99	2.01
9	0.10	0.80	0.09	0.00	0.00	2.01	0.00	0.99	2.01
10	0.08	0.81	0.10	0.00	0.00	2.00	0.00	1.00	2.00
11	0.11	0.79	0.09	0.00	0.00	2.02	0.00	0.98	2.02
12	0.02	0.89	0.08	0.02	0.00	1.98	0.01	1.01	1.99
13	0.07	0.82	0.10	0.00	0.00	2.01	0.00	0.99	2.01
14	0.04	0.91	0.04	0.00	0.00	2.01	0.00	0.99	2.01
15	0.07	0.86	0.06	0.00	0.00	2.01	0.00	0.99	2.01
16	0.12	0.65	0.20	0.00	0.00	1.93	0.10	0.97	2.03
17	0.02	0.95	0.02	0.00	0.00	2.01	0.00	0.99	2.01
18	0.13	0.74	0.11	0.00	0.00	1.94	0.07	0.98	2.02
19	0.04	0.93	0.02	0.00	0.00	2.02	0.00	0.98	2.02
20	0.15	0.70	0.14	0.00	0.00	1.93	0.09	0.99	2.01
21	0.03	0.93	0.02	0.00	0.00	2.02	0.00	0.98	2.02
22	0.12	0.74	0.13	0.00	0.00	1.96	0.06	0.98	2.02
23	0.03	0.94	0.02	0.00	0.01	2.00	0.00	1.00	2.00
24	0.03	0.94	0.02	0.00	0.01	2.00	0.00	1.00	2.00
25	0.05	0.85	0.08	0.00	0.01	2.01	0.00	0.99	2.01

Note. Results of quantitative SEM/EDS analyses are expressed in weight% and in values of atoms per formula unit (apfu) calculated for a total of 3 apfu; bdl: below detection limits. Results of analysis #3 include 0.66 wt % Cu (or 0.02 apfu). Relatively low totals are due to insufficient volumes of the analyzed grain.

3.2. Physical Properties of Tamuraite

The new mineral is gray to brownish gray in reflected light. It appears gray next to grains of Rh-rich pentlandite, which exhibits sharp and discrete boundaries with tamuraite (Figure 2a–d). The mineral is opaque with a metallic luster. Its bireflectance is very weak to absent. It is nonpleocroic to slightly pleochroic (grayish to light brown tints). It appears to be very weakly anisotropic (gray to light yellow tints). Reflectance values could not be measured because of insufficient grain sizes. Its streak was not observed, and the powder could not be extracted owing to the tiny grain size. The fluorescence, tenacity, magnetic properties and micro-indentation hardness also were not evaluated owing to the small grain size. The cleavage, parting, fracture and internal reflections were not observed. Density could not be measured owing to the small grain size.

The calculated value of density is 6.30 g·cm^{-3}; it is based on the unit-cell volume inferred from diffraction measurements and the empirical formula obtained for tamuraite in this study.

3.3. Chemical Composition of Tamuraite and the Tamuraite—Kuvaevite Series

Results of WDS analyses of tamuraite are listed in Table 4. The formula, $(Ir_{2.87}Rh_{1.75}Pt_{0.18}Ru_{0.01}Os_{0.01})_{\Sigma 4.82}(Fe_{4.41}Ni_{3.90}Cu_{1.87}Co_{0.02})_{\Sigma 10.20}S_{15.98}$, corresponds to the general formula $(Ir,Rh)_5(Fe,Ni,Cu)_{10}S_{16}$. The formula is recalculated based on 31 apfu by analogy with the Rh–(Ni)-dominant analog, i.e., torryweiserite (IMA2020-048) and with the Ni-dominant analog, i.e., kuvaevite (IMA2020-043) [15,16]. The total content of metals in the formula unit is 15.03 apfu. A minor amount of a Fe-site cation must be present at the Ir site to achieve the 1:2 stoichiometric proportion. The ideal formula of tamuraite is $Ir_5Fe_{10}S_{16}$, which requires Ir 47.28, Fe 27.48, and S 25.24, a total of 100 wt %.

Table 4. Compositions of tamuraite from the River Ko deposit in the Sisim Placer Zone.

#		Ir	Rh	Pt	Ru	Os	Fe	Ni	Cu	Co	S	Total (wt %)
1 *	27_2_33	30.68	8.95	1.43	0.03	0.04	13.21	12.13	6.36	0.07	27.25	100.16
2 *	27_3_3A	28.05	10.48	1.87	0.02	0.04	13.74	11.91	6.24	0.07	27.85	100.27
3	Mean	29.30	9.57	1.85	0.05	0.06	13.09	12.18	6.30	0.06	27.23	99.69
-	Range	27.75–30.68	8.46–10.71	1.43–2.10	0.02–0.07	0.03–0.13	12.38–13.74	11.78–13.12	6.06–6.56	0.04–0.07	26.14–27.89	-
-	Stand. Dev. (σ)	0.16	0.05	0.17	0.06	0.09	0.07	0.09	0.22	0.03	0.01	-
-	Standard	Pure Ir	Pure Rh	Pure Pt	Pure Ru	Pure Os	Pure Fe	Pentlandite	Pure Cu	Pure Co	Pentlandite	-

Atomic proportions based on a total of 31 apfu

#	Ir	Rh	Pt	Ru	Os	Σ	Fe	Ni	Cu	Co	Σ	ΣMe	S
1 *	3.00	1.63	0.14	0.01	<0.01	4.78	4.45	3.88	1.88	0.02	10.23	15.01	15.98
2 *	2.70	1.88	0.18	<0.01	<0.01	4.76	4.55	3.76	1.82	0.02	10.15	14.91	16.08
3	2.87	1.75	0.18	0.01	0.01	4.82	4.41	3.90	1.87	0.02	10.20	15.02	15.98

Note: Results of WDS analyses obtained using a JEOL JXA 8900L microprobe. * Composition (in wt %) of two grains of tamuraite investigated by synchrotron micro-Laue diffraction. Mean (#3) is the mean of six datasets.

The extent of Fe-for-Ni substitution is important, and tamuraite forms a well-established series of solid solutions with kuvaevite, ideally $Ir_5Ni_{10}S_{16}$, as is indicated by the WDS data from the River Ko suite (Figure 5). Tamuraite is the Fe-dominant member, and kuvaevite (IMA2020-043) [15] is the Ni-dominant member of the series; this inference is consistent with our results of the synchrotron-based microdiffraction studies. In addition, note that the type tamuraite has a composition that is the richest in Fe and is close to the end member in the inferred solid–solution series (Figure 5).

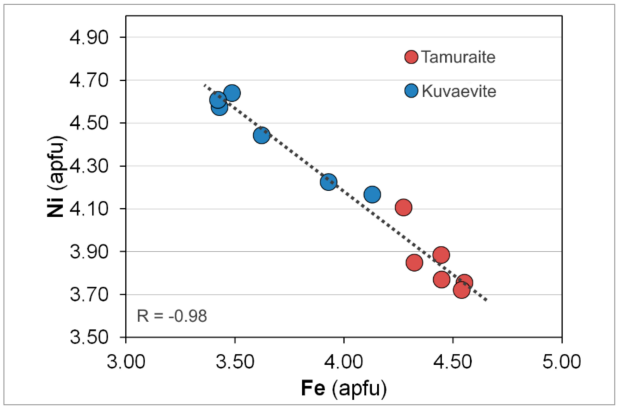

Figure 5. Inverse correlation of Fe vs. Ni (plotted in values of atoms per formula unit, apfu, calculated for a total of 31 apfu) in the composition of members of the tamuraite–kuvaevite series at River Ko, Eastern Sayans. Compositions of kuvaevite are based on specimens from the type locality [15].

3.4. Crystallography

The X-ray powder-diffraction data obtained using synchrotron micro-Laue diffraction are presented in Tables 5 and 6. The inferred crystal system is trigonal; the space group is $R\bar{3}m$ (#166). The calculated unit-cell parameters of tamuraite are a = 7.073(1) Å, c = 34.277(8) Å, V = 1485(1) Å^3, and Z = 3. The calculated c:a ratio is 4.8462. The space group $R\bar{3}m$ is implied by analogy with kuvaevite [15] and with torryweiserite, $Rh_5Ni_{10}S_{16}$, from the Marathon deposit, Coldwell complex, Ontario, Canada [16].

Table 5. X-ray powder-diffraction data (d in Å) for tamuraite.

h	k	l	d	I	h	k	l	d	I
0	0	3	11.4480	35.6	1	0	22	1.5128	5.6
1	0	1	6.0356	22.2	4	0	4	1.5089	3.2
1	**0**	**$\bar{2}$**	**5.7740**	**45.1**	4	$\bar{2}$	12	1.5053	4.9
0	0	6	5.7240	11.8	2	0	20	1.4982	3.8
1	0	4	4.9895	9.4	4	0	$\bar{5}$	1.4960	8.5
1	0	$\bar{5}$	4.5740	13.4	4	$\bar{1}$	11	1.4933	3.4
0	0	9	3.8160	13.6	4	0	$\bar{8}$	1.4435	7.2
2	$\bar{1}$	0	3.5398	12.0	0	0	24	1.4310	2.7
2	**0**	**$\bar{1}$**	**3.0534**	**43.2**	5	$\bar{2}$	$\bar{2}$	1.4019	4.3
2	**$\bar{1}$**	**6**	**3.0106**	**100.0**	4	$\bar{2}$	15	1.4003	4.5
1	**0**	**10**	**2.9963**	**50.0**	4	$\bar{1}$	14	1.3975	2.1
2	0	$\bar{4}$	2.8870	13.8	3	0	18	1.3947	2.4
0	0	12	2.8620	3.3	4	0	$\bar{11}$	1.3759	5.0
2	**0**	**5**	**2.7994**	**55.5**	5	$\bar{1}$	6	1.3028	16.3
1	0	$\bar{11}$	2.7822	12.2	5	$\bar{2}$	10	1.3016	6.7
2	0	$\bar{7}$	2.5998	8.0	3	$\bar{1}$	22	1.2947	5.3
2	**0**	**8**	**2.4948**	**37.9**	1	0	26	1.2913	3.8
3	$\bar{1}$	1	2.3121	3.8	5	$\bar{2}$	$\bar{11}$	1.2824	2.2
3	$\bar{1}$	$\bar{2}$	2.2965	4.3	2	0	25	1.2536	3.6
0	0	15	2.2896	3.0	4	0	16	1.2474	19.5

Table 5. *Cont.*

h	*k*	*l*	*d*	*I*	*h*	*k*	*l*	*d*	*I*
2	0	$\overline{10}$	2.2870	2.4	4	0	$\overline{17}$	1.2211	4.4
1	0	14	2.2776	4.2	4	$\bar{2}$	21	1.2011	9.1
3	$\bar{1}$	4	2.2373	3.5	2	$\bar{1}$	27	1.1971	2.8
3	$\bar{1}$	$\bar{5}$	2.1957	2.9	5	1	15	1.1551	2.5
2	0	11	2.1874	22.8	5	0	$\overline{10}$	1.1548	3.8
3	0	0	2.0437	2.5	4	$\bar{1}$	22	1.1500	4.1
3	0	6	1.9247	29.6	3	$\bar{1}$	26	1.1476	4.2
2	$\bar{1}$	15	1.9225	6.7	4	2	5	1.1425	2.1
3	1	10	1.9209	36.2	4	2	8	1.1186	2.1
3	$\bar{1}$	$\overline{11}$	1.8608	7.7	4	$\bar{2}$	24	1.1128	7.0
4	**$\bar{2}$**	**0**	**1.7699**	**71.0**	5	$\bar{1}$	18	1.0954	2.4
2	**0**	**16**	**1.7583**	**64.7**	5	$\bar{2}$	22	1.0450	3.7
4	$\bar{2}$	3	1.7491	2.9	4	$\bar{1}$	26	1.0432	3.7
4	$\bar{1}$	2	1.6922	4.5	4	$\bar{2}$	27	1.0329	3.2
4	$\bar{2}$	6	1.6909	2.8	4	2	16	1.0196	6.2
2	0	17	1.6869	13.0	2	0	32	1.0130	7.6
3	$\bar{1}$	$\overline{14}$	1.6846	6.7	5	2	6	0.9676	2.0
2	1	18	1.6796	4.0	5	$\bar{2}$	26	0.9629	3.2
0	0	21	1.6354	4.6	5	$\bar{1}$	27	0.9219	2.2
4	$\bar{2}$	9	1.6056	8.3	4	$\bar{2}$	33	0.8971	4.3
4	0	1	1.5312	6.3	4	4	0	0.8849	2.1
3	0	15	1.5247	3.0	4	0	32	0.8792	4.9
4	$\bar{1}$	$\overline{10}$	1.5239	14.4					

Note: Only reflections with $I \geq 2$ are listed. The strongest eight reflections are shown in bold.

Table 6. The characteristics of tamuraite compared with those of kuvaevite and torryweiserite.

#		Type Locality	Ideal Formula	Unit-Cell Parameters	Space Group	Reference
1	Tamuraite (grain 1) *	River Ko suite, Sisim Placer Zone, SW part of Eastern Sayans, Russia	$Ir_5Fe_{10}S_{16}$	a = 7.073 (1) Å c = 34.277 (8) Å V = 1485 (1) Å^3 and Z = 3	$R\bar{3}m$ (#166)	(This study)
2	Tamuraite (grain 2) **	River Ko suite	$Ir_5Fe_{10}S_{16}$	a = 7.090 (2) Å c = 34.387 (12) Å V = 1497 (1) Å^3 and Z = 3	$R\bar{3}m$ (#166)	(This study)
3	Kuvaevite	River Ko suite	$Ir_5Ni_{10}S_{16}$	a = 7.079 (5) Å c = 34.344 (12) Å V = 1490 (2) Å^3 and Z = 3	$R\bar{3}m$ (#166)	IMA2020-043; [15]
4	Torryweiserite	Marathon deposit, Coldwell complex, Ontario, Canada	$Rh_5Ni_{10}S_{16}$	a = 7.060(1) Å, c = 34.271(7) Å, V = 1479.3(1) Å^3, and Z = 3	$R\bar{3}m$ (#166)	IMA2020-048; [16]

Note: * 396 reflections indexed; ** 289 reflections indexed.

Tamuraite is considered isostructural with torryweiserite (Table 6). It is thus composed of three distinct layers of polyhedra that are stacked along [001]. By analogy with the structural motif and assignments worked out for torryweiserite [16], the first is a layer of $Ir1S_6$ octahedra sharing edges; it has octahedral voids, such as are found in dioctahedral micas. The second is a mixed layer composed of $Ir2S_6$ octahedra, $Fe1S_4$ and $Fe2S_4$ tetrahedra arranged in a pinwheel fashion, with $Ir2S_6$ at the center. The third layer consists of a double sheet of $Fe3S_4$ tetrahedra that share edges along [001] to form six-membered $Fe3S_4$ rings. The structure will be described in greater detail in the article on torryweiserite [16].

Among the compounds that are isotypic with tamuraite–kuvaevite and torryweiserite is synthetic $Cu_4Sn_7S_{16}$, which also crystallizes in space group $R\bar{3}m$ (#166), with a = 7.3788(2) Å, c = 36.032(2) Å, V = 1699(1) Å^3, and Z = 3. The structure of this sulfide contains distorted octahedra of CuS_6 and SnS_6, CuS_4 tetrahedra, and CuS_4 trigonal pyramids [17].

3.5. Etymology and Conservation

The mineral is named after Dr. Nobumichi Tamura (born 1966), senior scientist at the Advanced Light Source of the Lawrence Berkeley National Laboratory, Berkeley, California, to recognize his innovative investigations of minerals and materials by synchrotron microdiffraction. He is also recognized as one of the leading paleoartists, illustrators of the prehistoric denizens roaming the Earth.

The holotype specimen of tamuraite is deposited (catalog number: III-102/2) at the Central Siberian Geological Museum, Sobolev Institute of Geology and Mineralogy, Novosibirsk, Russia.

4. Discussion

4.1. Relation to Other Species

Tamuraite, $Ir_5Fe_{10}S_{16}$, is the Fe-dominant member in the tamuraite–kuvaevite solid–solution series with Fe > Ni, Fe > Cu, and Ir > Rh. Tamuraite is isostructural with kuvaevite [15] and with torryweiserite ($Rh_5Ni_{10}S_{16}$: IMA2020-048; McDonald et al.) (Table 6) [16].

Tamuraite is distinct from oberthürite ($Rh_3Ni_{32}S_{32}$), both compositionally and structurally; oberthürite is a member of the pentlandite group (with a = 10.066(5) Å) from the Marathon deposit, Coldwell complex, Ontario, Canada [16,18]. Tamuraite also differs, both compositionally and structurally, from ferhodsite [$(Fe,Rh,Ir,Ni,Cu,Co,Pt)_{9-x}S_8$] described at Nizhniy Tagil, Urals. The latter exhibits an Rh-enriched composition, with the dominance of Rh over Ir and other PGE, and has a tetragonal unit-cell ($P42/n$ or $P4/nmm$) with parameters a = 10.009(5) and c = 9.840(8) Å [19]. Members of the tamuraite—kuvaevite series are related to $Ir_5(Ni,Fe,Cu)_{10}S_{17.5}$ (not IMA-approved: Chairman's communication), from the Jicheng area, Luanhe River, China (a = b = 7.0745(14) Å and c = 34.267(10) Å; space group $R3m$: Yü et al. (2011) [20]. The reported composition of this phase can satisfactorily be recalculated to a tamuraite type of formula based on 31 apfu: $Ir_{4.96}(Ni_{4.31}Fe_{3.64}Cu_{1.52}Co_{0.27})_{\Sigma 9.75}S_{16.30}$.

Two separate series, i.e., the PGE-bearing pentlandite series and the ferhodsite series, were recently recognized in a representative set of global occurrences [2]. Based on our micro-Laue data and the latest structural results [16], we suggest that the latter series be renamed the torryweiserite series.

4.2. Provenance and Origin of Tamuraite

Our new results obtained for the tamuraite-bearing associations are consistent with a derivation from the Lysanskiy complex (Figure 1b) [3,4,21]. We contend that tamuraite and members of the tamuraite–kuvaevite–torryweiserite solid–solution series formed at an advanced stage of crystallization due to accumulation and buildup in sulfur in droplets of a residual melt enriched in S, Fe, Ni, Cu, and Rh. These elements were all essentially incompatible during the formation of the Os–Ir alloy in lode zones of chromitites (or Cr–Ti-rich zones) in the Lysanskiy layered complex. In the globules of melt trapped in the alloy host, tamuraite and laurite–erlichmanite, both enriched in Ir, likely crystallized

before the Rh-rich pentlandite poor in Ir. This sequence is consistent with evolutionary paths established for the Ni–Fe–(Co)–PGE sulfarsenide droplets, which developed with a core-to-rim decrease in their values of the Ir# index, i.e., 100 Ir/(Ir + Rh) [12,22].

Author Contributions: The authors wrote the article together. A.Y.B.: investigations, conclusions, writing; N.D.T.: investigations, sampling, writing; R.F.M.: discussions, conclusions, writing; A.M.M.: discussions, conclusions. All authors have read and agreed to the published version of the manuscript.

Funding: This research was supported by the Russian Foundation for Basic Research (project # RFBR 19-05-00181).

Institutional Review Board Statement: Not applicable.

Informed Consent Statement: Not applicable.

Data Availability Statement: Additional data are available from the corresponding author upon a reasonable request or query.

Acknowledgments: We thank Nobumichi Tamura for his expert assistance with the results of synchrotron X-ray studies of tamuraite. We are grateful to Lang Shi and Nikolai S. Karmanov for their help with the WDS EMP and SEM-EDS analyses. We also thank the three anonymous referees and editors for their helpful comments. This study was carried out within the framework of the state assignment of the VS Sobolev Institute of Geology and Mineralogy of the Siberian Branch of the Russian Academy of Sciences (financed by the Ministry of Science and Higher Education of the Russian Federation).

Conflicts of Interest: The authors declare no conflict of interest.

References

1. Tolstykh, N.D.; Krivenko, A.P. On the composition of sulfides containing the platinum-group elements. *Zap. Vses. Mineral. O-va* **1994**, *123*, 41–49. (In Russian)
2. Barkov, A.Y.; Shvedov, G.I.; Nikiforov, A.A.; Martin, R.F. Platinum-group minerals from Seyba, Eastern Sayans, Russia, and substitutions in the PGE-rich pentlandite and ferhodsite series. *Mineral. Mag.* **2019**, *83*, 531–538. [CrossRef]
3. Barkov, A.Y.; Shvedov, G.I.; Martin, R.F. PGE–(REE–Ti)-rich micrometer-sized inclusions, mineral associations, compositional variations, and a potential lode source of platinum-group minerals in the Sisim Placer Zone, Eastern Sayans, Russia. *Minerals* **2018**, *8*, 181. [CrossRef]
4. Bezzubtsev, V.V. (Ed.) *The State Geological Map of the Russian Federation Scale 1: 1 000 000 (The Third Generation)*; (Altai-Sayan Series N-46 Abakan; The explanation notes); The Ministry of Natural Resources and Environment of the Russian Federation, "RosNedra", A.P. Karpinsky Russian Geological Research Institute (VSEGEI), and "Krasnoyarskgeolsyomka": Saint Petersburg, Russia, 2008; p. 391.
5. Nesterenko, G.V.; Zhmodik, S.M.; Belyanin, D.K.; Airiyants, E.V.; Karmanov, N.S. Micrometric inclusions in platinum-group minerals from Gornaya Shoria, southern Siberia, Russia: Problems and genetic significance. *Minerals* **2019**, *9*, 327. [CrossRef]
6. Tamura, N. XMAS: A Versatile Tool for Analyzing Synchrotron X-ray Microdiffraction Data. In *Strain and Dislocation Gradients from Diffraction*; Barabash, R., Ice, G., Eds.; Imperial College Press: London, UK, 2014; pp. 125–155.
7. Harris, D.C.; Cabri, L.J. Nomenclature of platinum-group-element alloys: Review and revision. *Can. Mineral.* **1991**, *29*, 231–237.
8. Knop, O.; Huang, C.-H.; Reid, K.I.G.; Carlow, J.S. Chalcogenides of the transition elements. X. X-ray, neutron, Mössbauer and magnetic studies of pentlandite and the π phases, π (Fe, Co, Ni, S), Co_8MS_8 and $Fe_4Ni_4MS_8$ (M = Ru, Rh, Pd). *J. Solid State Chem.* **1976**, *16*, 97–116. [CrossRef]
9. Barkov, A.Y.; Shvedov, G.I.; Silyanov, S.A.; Martin, R.F. Mineralogy of platinum-group elements and gold in the ophiolite-related placer of the River Bolshoy Khailyk, Western Sayans, Russia. *Minerals* **2018**, *8*, 247. [CrossRef]
10. Cabri, L.J.; Laflamme, J.H.G. Analyses of minerals containing platinum-group elements. In *Platinum-Group Elements: Mineralogy, Geology, Recovery*; Cabri, L.J., Ed.; Canadian Institute of Mining, Metallurgy and Petroleum (CIM): Montreal, QC, Canada, 1981; Special Volume 23, pp. 151–173.
11. Cabri, L.J. (Ed.) *The Geology, Geochemistry, Mineralogy, Mineral Beneficiation of the Platinum-Group Elements*; Canadian Institute of Mining, Metallurgy and Petroleum, (CIM): Montreal, QC, Canada, 2002; Special Volume 54, p. 852.
12. Barkov, A.Y.; Fleet, M.E.; Martin, R.F.; Alapieti, T.T. Zoned sulfides and sulfarsenides of the platinum-group elements from the Penikat layered complex, Finland. *Can. Mineral.* **2004**, *42*, 515–537. [CrossRef]
13. Barkov, A.Y.; Tolstykh, N.D.; Shvedov, G.I.; Martin, R.F. Ophiolite-related associations of platinum-group minerals at Rudnaya, western Sayans, and Miass, southern Urals, Russia. *Mineral. Mag.* **2018**, *82*, 515–530. [CrossRef]

14. Cabri, L.J.; Harris, D.C.; Weiser, T.W. Mineralogy and distribution of platinum-group mineral (PGM) placer deposits of the world. *Explor. Min. Geol.* **1996**, *5*, 73–167.
15. Barkov, A.Y.; Tolstykh, N.D.; Tamura, N.; Martin, R.F.; Ma, C. Kuvaevite, IMA 2020-043, in: CNMNC Newsletter 58. *Eur. J. Mineral.* **2020**, *32*. [CrossRef]
16. McDonald, A.M.; Kjarsgaard, I.; Cabri, L.J.; Ross, K.C.; Ames, D.E.; Bindi, L.; Good, D.J. Oberthürite, $Rh_3(Ni,Fe)_{32}S_{32}$, and torryweiserite, $Rh_5Ni_{10}S_{16}$, two new platinum-group minerals from the Marathon deposit, Coldwell complex, Ontario, Canada: Descriptions, crystal chemical considerations and comments on the geochemistry of rhodium. *Can. Mineral.* **2021**, *59*, in press.
17. Jemetio, J.P.F.; Zhou, P.; Kleinke, H. Crystal structure, electronic structure and thermoelectric properties of $Cu_4Sn_7S_{16}$. *J. Alloys Compd.* **2006**, *417*, 55–59. [CrossRef]
18. McDonald, A.M.; Kjarsgaard, I.M.; Ross, K.C.; Ames, D.E.; Cabri, L.J.; Good, D.J. Oberthürite, IMA 2017-072. CNMNC Newsletter No. 40, December 2017, p. 1579. *Mineral. Mag.* **2017**, *81*, 1577–1581.
19. Begizov, V.D.; Zavyalov, E.N. Ferhodsite (Fe,Rh,Ir,Ni,Cu,Co,Pt)$_{9-x}S_8$—A new mineral from the Nizhniy Tagil ultramafic complex. *New Data Minerals* **2016**, *51*, 8–11. (In Russian)
20. Yü, Z.; Hao, Z.; Wang, H.; Yin, S.; Cai, J. Jichengite, $3CuIr_2S_4 \cdot (Ni,Fe)_9S_8$, a new mineral, and its crystal structure. *Acta Geol. Sin.* **2011**, *85*, 1022–1027. [CrossRef]
21. Glazunov, O.M. *The Geochemistry and Petrology of the Gabbro-Pyroxenite Formation of the Eastern Sayans*; Nauka: Novosibirsk, Russia, 1975; p. 188. (In Russian)
22. Barkov, A.Y.; Thibault, Y.; Laajoki, K.V.O.; Melezhik, V.A.; Nilsson, L.P. Zoning and substitutions in Co–Ni–(Fe)–PGE sulfarsenides from the Mount General'skaya layered intrusion, Arctic Russia. *Can. Mineral.* **1999**, *37*, 127–142.